



## Agar hydrogel supported metal nanoparticles catalyst for pollutants degradation in water

Tahseen Kamal<sup>a,\*</sup>, Ikram Ahmad<sup>a,b,c</sup>, Sher Bahadar Khan<sup>a,b</sup>, Abdullah M. Asiri<sup>a,b</sup>

<sup>a</sup>Department of Chemistry, Faculty of Science, King Abdulaziz University, P.O. Box 80203, Jeddah 21589, Saudi Arabia, emails: tkkhan@kau.edu.sa (T. Kamal), ravian\_611855@hotmail.com (I. Ahmad), dr.khanchemist@gmail.com (S.B. Khan), aasiri2@kau.edu.sa (A.M. Asiri)

<sup>b</sup>Center of Excellence for Advanced Materials Research, King Abdulaziz University, P.O. Box 80203, Jeddah 21589, Saudi Arabia

<sup>c</sup>Department of Applied Chemistry, Government College University, Faisalabad-38000, Pakistan

Received 8 February 2018; Accepted 30 September 2018

### ABSTRACT

In this study, agar hydrogel (AG) was prepared and used as support for the copper and cobalt nanoparticles inside it. AG hydrogels at three different concentrations of 0.4, 1 and 2 wt/wt% were prepared by cooling down their aqueous solutions to room temperature. All these hydrogels were separately introduced into the 0.5 M copper sulphate or cobalt chloride aqueous solutions to uptake the respective metal ions. The ions loaded hydrogels were treated with concentrated  $\text{NaBH}_4$  aqueous solution to prepare the copper or cobalt nanoparticles loaded AG hydrogels (Cu-AG or Co-AG). Pure AG as well as  $\text{M}^{2+}$ -AG hydrogels were characterized using various instrumental techniques such as field emission scanning electron microscope, thermogravimetric analysis, and X-ray diffraction. Finally, the  $\text{M}^{2+}$ -AG hydrogels were utilized as catalysts in methylene blue dye reduction reaction using  $\text{NaBH}_4$  as reducing agent.

**Keywords:** Agar; Hydrogel; Copper nanoparticles; Cobalt nanoparticles; Catalyst

### 1. Introduction

Over the past two decades, nanoparticles have drawn extensive research attention from scientific community due to their extensive utilization in different fields, that is, sensors, biomedical field and catalysis [1–7]. Specifically, the field of catalysis is completely dependent on use of various kinds of metal-based catalysts [2,8,9]. Since catalysis is surface-related phenomenon, catalysts with dimensions in nanoscale (nanoparticles) display highest surface area and hence highest catalytic properties as compared with their bulk materials [10,11]. To date, most of the transition metal based nanoparticle catalysts have been recognized to show high catalytic characteristics [12,13]. However, such high catalytic properties decline with the passage of time due to aggregation of the nanoparticles which reduces their surface area [14]. In the effort of giving long-term stabilities and maximum operating time to the nanoparticles, different strategies

were used. These include the utilization of block copolymers, surfactants and both rigid and soft materials based supports [12,15–17]. Among transition metals, noble metals based catalysts have been widely explored for catalysis but their high cost is the main hurdle to be applied in actual field. However, herein, we rely on the preparation of comparatively low cost heavy transition metals of copper and cobalt nanoparticles for use in catalysis.

Among the soft nature catalytic supports, the polymers are most commonly used supports because of their easy processability [18]. For instance, Kamal et al. [4] used microfibrinous form of the cellulose polymer for immobilization of the silver nanoparticles for the reduction of MB dye in aqueous solution. Recently, we used cellulose based catalytic supports in different studies. It was shown that the high catalytic properties were retained for few cycles. For the aqueous based reactions, Sahiner [12] suggested the use of synthetic polymer hydrogels. Various novel polymers based hydrogels were

\* Corresponding author.

introduced. However, the uncommon nature of the monomers and laborious methods of polymerization need to be replaced with other naturally available polymer hydrogels. For this purpose, Thomas et al. [19] used alginate/carboxymethyl cellulose/TiO<sub>2</sub> nanocomposite hydrogel for the photocatalytic degradation of the Congo red dye. Firouzabadi et al. [20] used agarose hydrogel immobilized Pd nanoparticles as recyclable catalyst for Suzuki–Miyaura reaction in aqueous media. In fact, there are numerous studies concerning the preparation of the biopolymer-based hydrogel nanocomposite with metal nanoparticles but the product was used for some other purposes [21]. Therefore, there is a huge potential of using other biopolymer-based hydrogels such as agar as support for the immobilization of metal nanoparticles.

Besides the importance of catalysts for the catalysis of various important organic synthesis, these are widely used in the elimination of the organic dyes from water bodies by process of reduction [1,4,22]. A large portion of synthetic organic dyes are used worldwide in textile industries. Some of these dyes, being water soluble, are discharged into the water streams to get rid of them. However, these dyes impose adverse effects directly on the aquatic life and indirectly on human beings [17,23]. Therefore, the effluents must be processed prior to their discharge into the water bodies. Since, other methods such as adsorption are time consuming and slow process and also some secondary processing like the requirement of regeneration of the adsorbents appeal to use other effective process such as catalytic reduction [24,25].

In this article, we prepared agar based hydrogels. The turbid suspensions of agar in water were heated in microwave oven for 2 min which resulted in agar dissolution. The hot agar solutions were put into glass petri dishes where it turned into hydrogels upon cooling. The hydrogels were cut into different shapes and put into Cu and Co salt solutions, separately. After absorption of sufficient amount of the ions, the hydrogels were treated with sodium borohydride solution which resulted in nanoparticles generation from the reduction and accumulation of the absorbed metal ions. The nanoparticles loaded hydrogels were characterized using different spectroscopic techniques and used in catalyzing the methylene blue (MB) dye reduction using NaBH<sub>4</sub>.

## 2. Experimental

### 2.1. Materials

Agar polymer was purchased from Japan. It has 9.0% agarose. Sodium borohydride (NaBH<sub>4</sub>, 99%) was purchased from BDH chemicals, Poole, England. Organic dye of methylene blue (C<sub>16</sub>H<sub>18</sub>ClN<sub>3</sub>S, 319.85 g/mol) was kindly supplied by Chemical Engineering Department, King Saud University, Riyadh, Saudi Arabia. Copper sulphate and cobalt chloride salts were obtained from BDH chemicals, Poole, England. Ultrapure water (>18 Ω) was used for the solutions preparation.

### 2.2. Hydrogels preparation

Hydrogels were prepared by dissolution of the agar polymer in water followed by thermal crosslinking. Briefly, 1 g of agar was put into a beaker containing 50 mL de-ionized water. It was stirred for 2 min which resulted in the turbid

suspension of the polymer in water. The suspension was then kept in a household microwave oven (Hyundai, South Korea) and heated for 2 min with alternate 5 s on and off cycle. Microwave heating treatment of the agar suspension resulted in the dissolution of the polymer as it became clear from initial turbid state. The boiled agar solution was then poured into clean glass petri dishes and kept static for 30 min at 20°C. The clear solution was formed into gel upon cooling which was cut into desired pieces for further use. Similarly, two more hydrogels were prepared with the agar concentrations in water of 0.4 and 1 wt%.

### 2.3. Nanoparticles preparation inside hydrogels

In order to prepare nanoparticles inside hydrogels, two aqueous solutions of Cu and Co were separately prepared. The concentrations of both the solutions were 0.5 M.

Each agar hydrogel with metal nanoparticles was named as M-AGxx where M stands for metal (Cu or Co), AG represents agar and xx denotes the wt% of the agar solution from which the hydrogel was prepared. For instance, Cu-AG0.4 indicates Cu nanoparticles loaded agar hydrogel produced from 0.4 wt% agar solution.

### 2.4. Catalytic experiments

The catalytic activity of the M-AGxx was evaluated in the methylene blue (MB) dye reduction using NaBH<sub>4</sub> at room temperature. A desired M-AGxx hydrogel with a constant weight of 0.23 g was cut and added to a quartz cuvette containing 3 mL MB dye. The M-AG hydrogel was meshed before adding to the cuvette. The reaction was initiated by the addition of freshly prepared 1 mL of 0.2 M NaBH<sub>4</sub> aqueous solution to the dye containing cuvette. The cuvette was placed in a UV-visible spectrophotometer and absorbance spectra were recorded after constant interval of time until the complete disappearance of the solution color.

### 2.5. Characterizations

Sample's surface morphology was examined using field emission scanning electron microscope (FESEM) instrument FE-SEM, JEOL JSM-7600F, Japan. Hydrogel samples were kept in freeze drier and freeze dried prior to the FESEM analysis. The as-obtained freeze dried samples were Pt coated for 10 s using JEOL, JEC-1600 auto fine coater prior to SEM observations. X-ray diffraction (XRD) analysis was performed using Thermo Scientific, ARL X'tra X-ray diffractometer. The XRD instrument was operated at 40 kV and 50 mA which produced X-rays with 0.1542 nm wavelength. The data were acquired at 2° 2θ min<sup>-1</sup>. Thermogravimetric analysis (TGA) was performed using TA Q500 instrument. In a typical experiment, sample was heated in an aluminum pan in the range of 25°C–700°C. A Thermo Scientific Evolution 300 UV-visible spectrophotometer was used for the measurement of the absorbance spectra.

## 3. Results and discussion

Fig. 1 represents the preparation procedure of the Cu-AGxx and Co-AGxx catalysts. Briefly, agar powder was suspended in a deionized water with final concentrations of

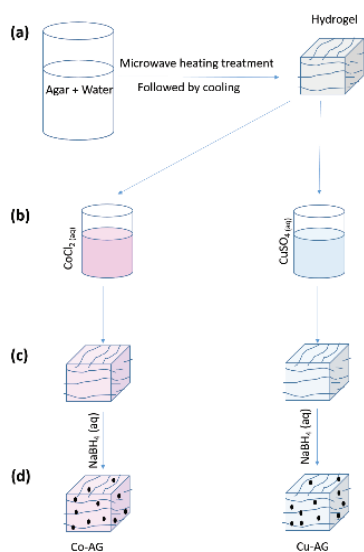


Fig. 1. Preparation of M-AGxx catalyst. (a) AG hydrogel preparation, (b) salt solutions treatment, (c) corresponding ions absorbed AG hydrogels and (d)  $\text{NaBH}_4$  treatment of the M-AGxx.

0.4, 1 and 2 wt%. All these suspensions were heated until they became clear. The boiled clear solutions were poured into petri dishes and cooled to room temperature for hydrogel formation. The prepared hydrogels were incorporated into either aqueous  $\text{CoCl}_2$  or  $\text{CuSO}_4$  solution for the metal ions uptake. Hydrogels were retained inside metal salt solutions for 24 h for the maximum uptake of the  $\text{M}^{2+}$  ions. The  $\text{M}^{2+}$ -AGxx were first finely meshed and then treated with  $\text{NaBH}_4$  aqueous solution to prepare the M-AGxx catalyst.

Hydrogel samples' morphology was examined by FESEM technique. Fig. 2 shows the morphological features of the agar hydrogel. Hydrogels were first freeze dried and coated with Pt prior for the FESEM analyses. The naked eye observation of the samples suggests a porous morphology. All the samples had sponge-like texture. The sizes of pores were in the range of millimeter to sub-millimeter diameter. The sizes of the pores in each specific sample were not uniform throughout the sample. We also observed that the AG0.4 and AG01 collapsed during the freeze drying process. The FESEM image of AG02 suggests that it had additional pores sizes in the range of 30–150  $\mu\text{m}$ . General overview of the literature suggests that the increasing concentration of polymer results in the small pore size. Fig. 2(c) represents the EDX spectrum of the sample which confirms that it was composed of only organic components.

Further we examined the dried Cu-AG02 and Co-AG02 by FESEM. Upon drying the M-AG02 hydrogels, it lost the initial dark black color. Probably, the oxidation of the metal nanoparticles caused such changes. Figs. 3(a) and (b) represent the FESEM images of Cu-AG02 at low and high magnifications, respectively. Similarly, Figs. 3(d) and (e) represent the FESEM images of Co-AG02 at low and high magnifications, respectively. In the low magnification images, pores can be observed. High magnification images also show the corresponding metal nanoparticles. Since the nanoparticles were very small, further high magnification images were not obtained. Focusing of the beam on sample surface for

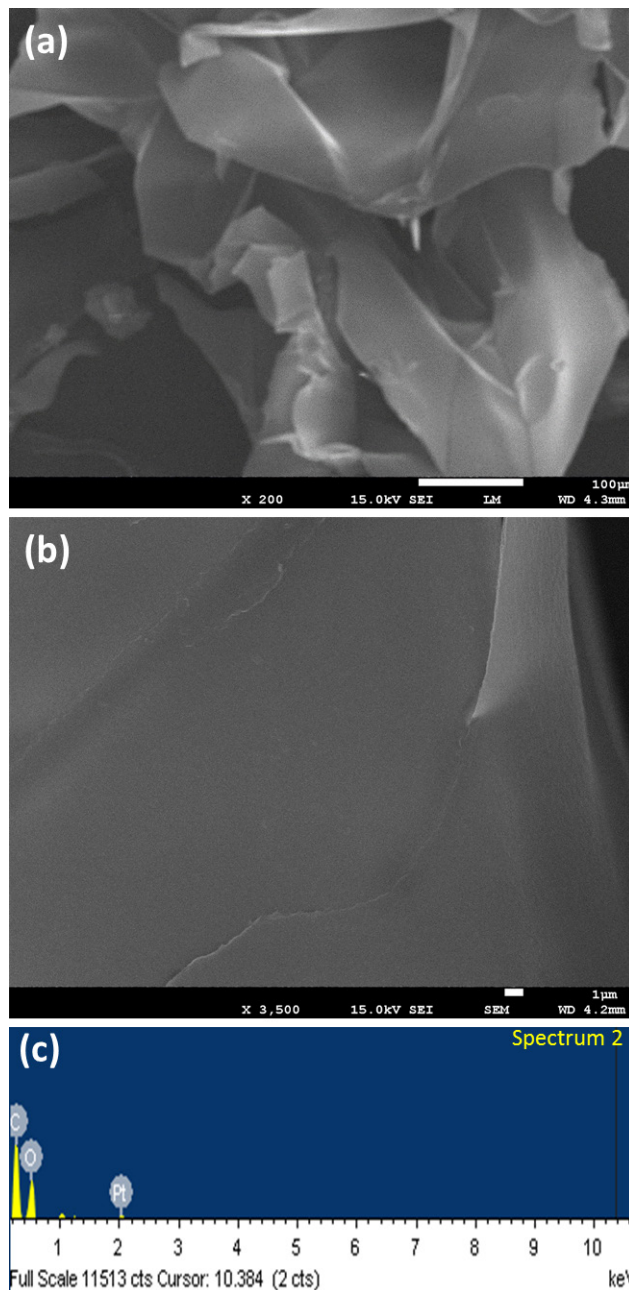


Fig. 2. Typical FESEM images of AG01 (a) at low magnification, (b) at high magnification and (c) corresponding SEDX spectrum.

the high magnification image was resulting in the burning of the sample. EDX analysis was performed for the presence of nanoparticles and their quantity. Figs. 3(c) and (f) show the EDX spectra of the Cu-AG02 and Co-AG02, respectively. The peaks of the Cu and Co in these spectra indicate that the samples had corresponding metal nanoparticles.

### 3.1. TGA

Fig. 4(A) shows XRD patterns of AG02, Cu-AG02 and Co-AG02. The XRD pattern of pure AG02 had a single broad peak. This peak at  $2\theta = 19^\circ$  represents the amorphous nature of the sample. The XRD patterns of Cu-AG02 and Co-AG02

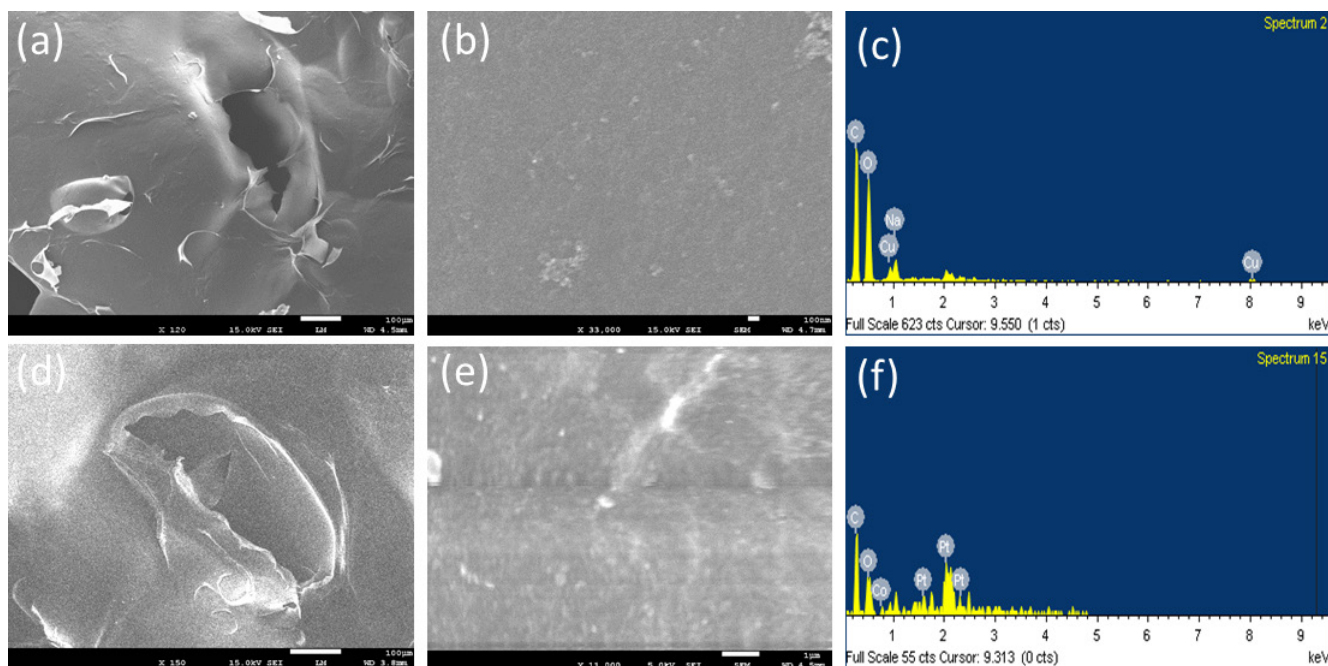


Fig. 3. FESEM images of Cu-AG02 (a) at low magnification, (b) at high magnification and (c) corresponding SEDX spectrum, and FESEM images of Co-AG02 (a) at low, (b) at high magnification and (c) corresponding SEDX spectrum.

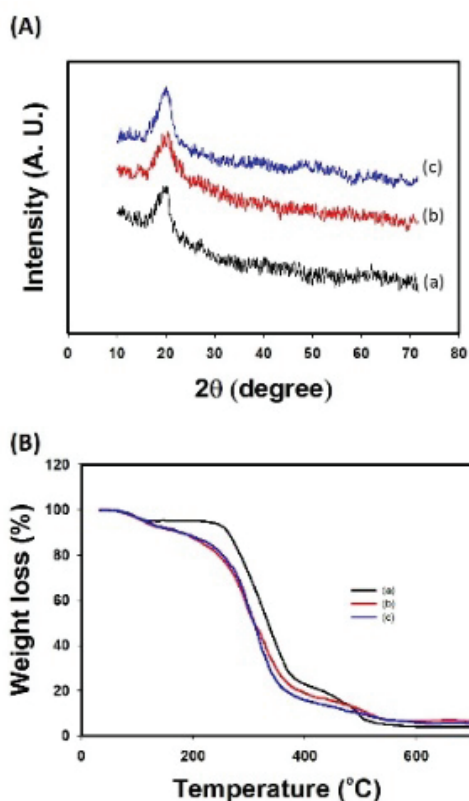


Fig. 4. XRD patterns (A) and TGA thermograms (B) of AG02 (a), Cu-AG02 (b) and Co-AG02 (c).

were similar to the pure AG02. Except the presence of peak at  $2\theta = 19^\circ$ , no other peak was observed in the XRD patterns of Cu-AG02 and Co-AG02. These results suggest that

as-prepared copper and cobalt nanoparticles were not crystalline in nature. It has been reported that annealing at high temperature is usually required for enhancing the crystallinity in the nanoparticles.[26] Another reason for the absence of the peaks of metallic nanoparticles might be their low concentration in the samples. Fig. 4(B) shows TGA thermograms of AG02, Cu-AG02 and Co-AG02. The initial weight loss around  $100^\circ\text{C}$  in the AG02 thermogram was due to moisture loss in the samples. The next high mass loss was due to the degradation of the agar and polyglycerol.

### 3.2. Catalytic experiments

Before proceeding to the actual catalytic experiments, adsorption study of MB from its aqueous solution on the pure AG hydrogels was performed. Figs. S1(a)–(c) show the UV-visible absorbance spectra of MB dye aqueous solutions before and after the introduction of 0.23 g of each hydrogel. In all cases, it can be clearly observed that the peak intensity at 660 nm decreased after putting the hydrogel sample in 3 mL of 0.05 mM MB. This decrement was considered due to the MB dye uptake by the hydrogel. The extent of the decrement of the peak 660 nm can be attributed to the MB amount uptake by the hydrogel. Fig. S1(d) show the amount (%) of the MB adsorbed on the corresponding hydrogel sample after taking it out after a period of 24 h. The MB amount adsorbed on the 0.4, 1 and 2 wt% AG was 19.08%, 32.70% and 43.09%.

Fig. 5 shows time-dependent absorbance spectra of MB dye aqueous solution after introducing  $\text{NaBH}_4$  aqueous solution and Cu-AG0.4, Cu-AG01 and Cu-AG02 catalysts. The main peak was constant in the absence of catalyst because the reaction did not occur. However, the peak located at 660 nm started to decrease upon introducing Cu-AG0.4 catalyst. Such a reduction in the absorbance was considered from the

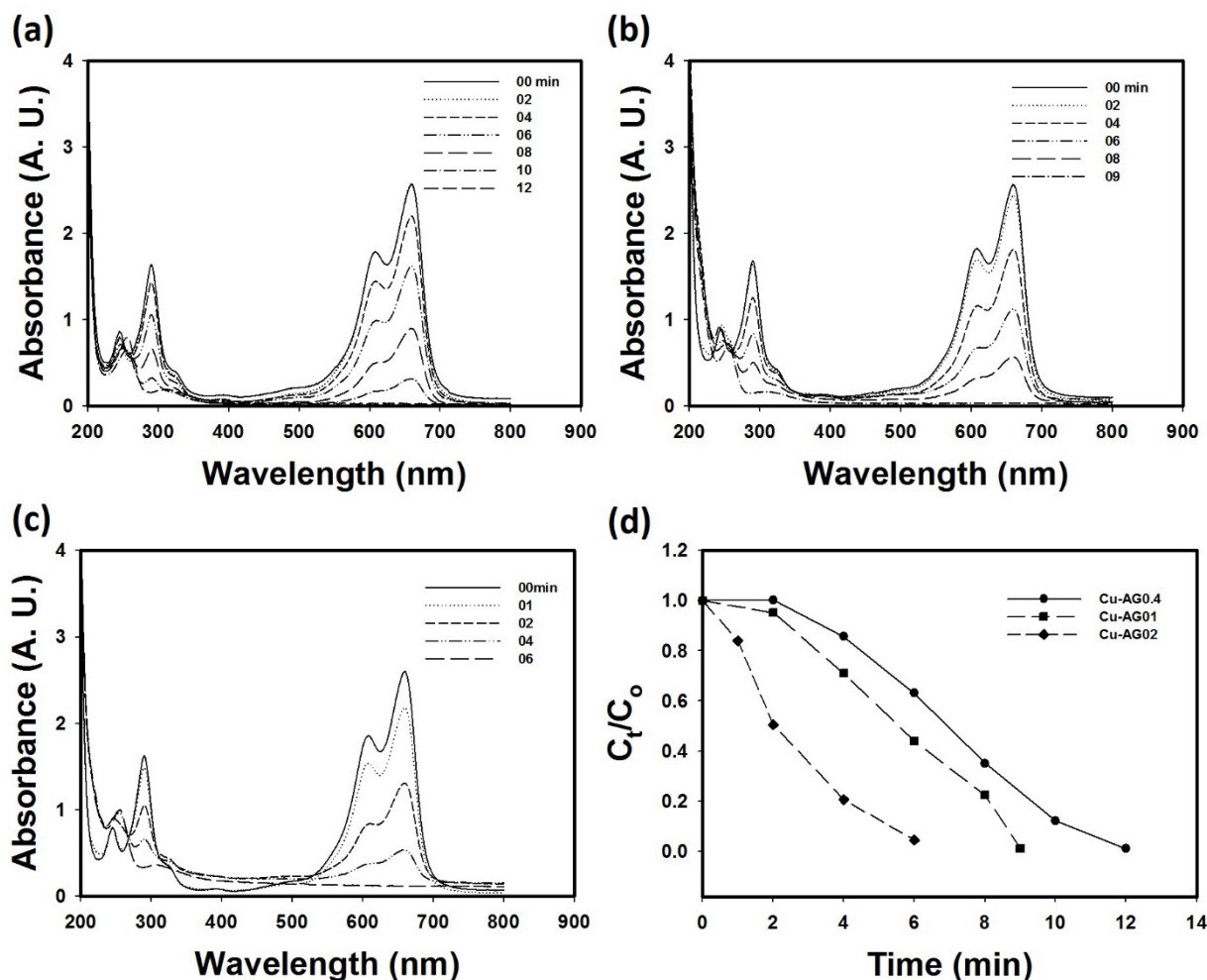


Fig. 5. Time-dependent absorbance spectra of MB dye aqueous solution after introducing (a) Cu-AG0.4, (b) Cu-AG01 and (c) Cu-AG02. The corresponding  $C_t/C_0$  vs. time plot (d). Experimental conditions were 2 mL [MB] = 0.05 M, 1 mL [ $\text{NaBH}_4$ ] = 0.1 M and 0.23 M-AG catalyst.

reduction of the MB molecules. The characteristic peak of the MB at 660 nm disappeared completely after 12 min. The time to complete the reduction reaction of MB in the presence of Cu-AG01 and Cu-AG02 were 9 and 6 min, respectively. In the catalytic reduction reaction of dyes, the application of metal nanoparticles as catalyst is to transfer the electron from the  $\text{BH}_4^-$  donor to the dye molecules through their mutual adsorption on the surface of nanocatalyst [22,27]. Another school of thought is that the catalyst acts as electron storage during the electron transfer process [28]. In the present case, 0.23 g of each Cu nanoparticles loaded hydrogel was used as catalyst. The fact is that the actual catalytic nanoparticles were more with the increasing concentration of the AG hydrogel. Therefore, the expected number of nanoparticles could be high in Cu-AG02 as compared with the Cu-AG0.4 and Cu-AG01. Thus the collective high surface area of the Cu nanoparticles in Cu-AG02 was responsible for the quick reduction process of the MB dye molecules. To determine the kinetic parameters using first-order reaction rate, the data from Figs. 5(a)–(c) was plotted as shown in Fig. 5(d). The calculated rate of reactions using Cu-AG0.4, Cu-AG01 and Cu-AG02 were 0.0934, 0.1135 and 0.1639  $\text{min}^{-1}$ , respectively.

Similarly, we performed the MB catalytic reduction reaction using Co nanoparticles loaded AG hydrogels of Co-AG0.4, Co-AG01 and Co-AG02. In order to avoid the repetition of the plots, the UV-visible absorbance spectra where the Co-AGxx catalysts were used are not shown here. Fig. 6 shows the  $C_t/C_0$  vs. time plot for the MB reduction reaction using 0.23 g of Co-AG0.4, Co-AG01 and Co-AG02. The trend of the MB reduction reaction catalyzed by Co nanoparticles loaded AG hydrogels was similar to that of the Cu-AGxx. The calculated rate of reactions using Co-AG0.4, Co-AG01 and Co-AG02 was 0.081, 0.129 and 0.187  $\text{min}^{-1}$ , respectively.

Further the effect of dye concentration on the rate of reduction reaction was evaluated. MB dye concentrations of 0.01, 0.05 and 0.1 mM were used in these reactions. A constant volume of 1 mL  $\text{NaBH}_4$  with a concentration of 0.1 M was used. Both the catalysts of Cu-AG02 and Co-AG02 were tested in these reactions. Fig. 7 shows  $C_t/C_0$  vs. time plot for the MB reduction reaction using 0.23 g of (a) Cu-AGxx and (b) Co-AGxx. The calculated rates of reduction reactions were 0.0624, 0.1332 and 0.1639  $\text{min}^{-1}$ , using Cu-AG0.4, Cu-AG01 and Cu-AG02, respectively. Similarly the rate

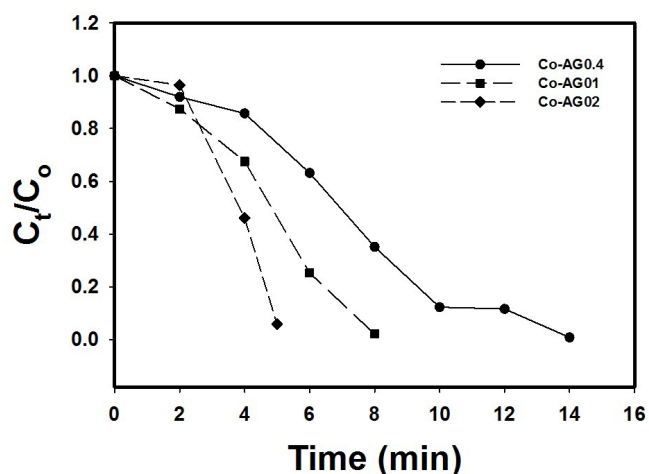


Fig. 6.  $C_t/C_o$  vs. time plot for the MB reduction reaction using 0.23 g of Co-AG0.4, Co-AG01 and Co-AG02.

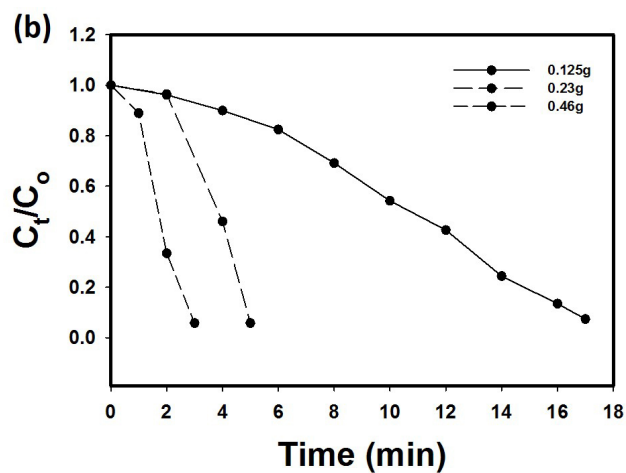
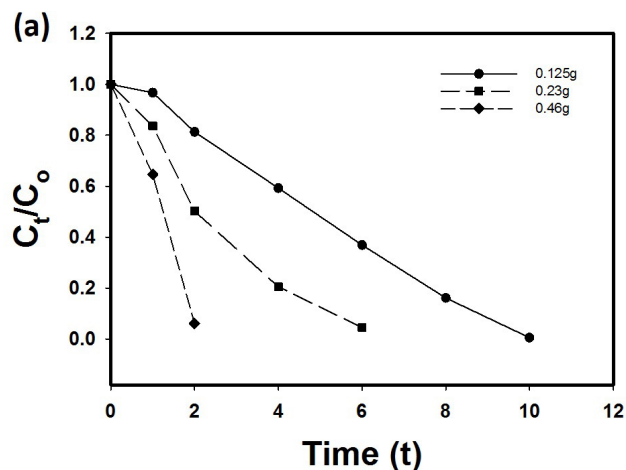


Fig. 8. Effect of the amount of the catalyst on the reduction reaction of MB.  $C_t/C_o$  vs. time plot for the MB reduction reaction using indicated amounts of (a) Cu-AG02 and (b) Co-AG02. The other conditions of the reactions were 1 mL of 0.1 M  $\text{NaBH}_4$  and 3 mL of the 0.05 M MB dye concentration.

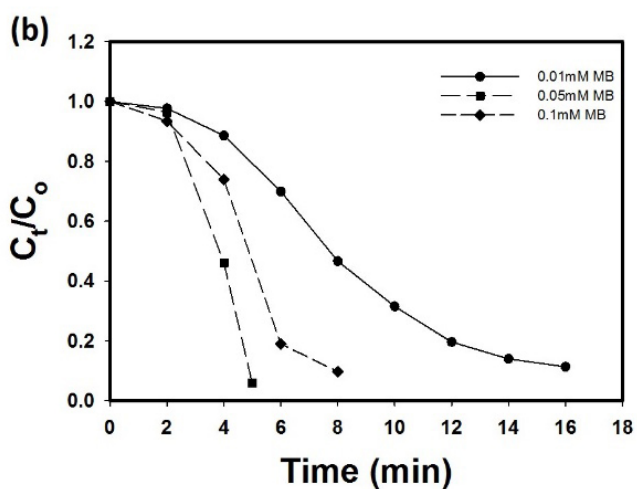
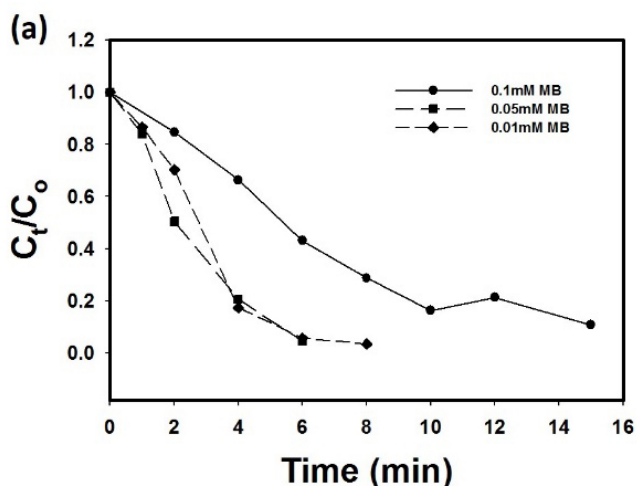


Fig. 7. Effect of MB dye concentration on the reduction reaction of MB.  $C_t/C_o$  vs. time plot for the MB reduction reaction using 0.23 g of (a) Cu-AGxx and (b) Co-AGxx while using the dye concentrations of 0.01, 0.05 and 0.1 mM in the presence of 0.1 M  $\text{NaBH}_4$ .

of reduction reactions was 0.0652, 0.1275 and 0.1875  $\text{min}^{-1}$ , using Co-AG0.4, Co-AG01 and Co-AG02, respectively. All these results are in line with those obtained by Sahiner [12] where upon increasing the concentration of the dye resulted in the slower reduction and thus the decreased reaction rate constant [29].

The effect of varying the catalyst amount was also evaluated on the MB dye reduction rate reaction. The Cu-AG02 and Co-AG02 catalyst amounts were varied as 0.125, 0.23 and 0.46 g. All other reaction conditions were kept constant. Figs. 8(a) and (b) show the  $C_t/C_o$  vs. time plot for the MB reduction reaction using 0.23 g of Cu-AG02 and Co-AG02 catalysts. Obviously, the rate of reaction was found to be faster upon increasing the catalyst amount. This was due to the increased surface area of the catalyst upon increasing its amount. We also compared our results with some of the available reports concerning the MB degradation as shown in Table 1. It can be observed in Table 1 that Cu-AG02 and Co-AG02 could compete with some of the catalysts.

Table 1

Comparison of the Cu-AG02 and Co-AG02 performance with the reported catalysts

Catalyst name	Type of catalyst	Rate constant (min <sup>-1</sup> )	Reference
Crosslinked poly(tannic acid)-Cu	Ordinary with NaBH <sub>4</sub>	0.68	[30]
Poly-o-phenylenediamine modified TiO <sub>2</sub> nanocomposite	Photocatalyst	0.0033	[31]
Fe-chitosan coated cotton cloth	Ordinary with NaBH <sub>4</sub>	0.2802	[32]
TiO <sub>2</sub> -pillared HTaWO <sub>6</sub>	Photocatalyst	0.053	[33]
Cu-AG02	Ordinary with NaBH <sub>4</sub>	0.1639	This study
Co-AG02	Ordinary with NaBH <sub>4</sub>	0.1875	This study

#### 4. Conclusion

In summary, agar hydrogel containing transition metals of copper and cobalt nanoparticles were successfully prepared. The prepared materials were characterized using FESEM, XRD and TGA. The pore size increased with the decreasing concentration of the initial agar suspension. XRD revealed that the nanoparticles were amorphous in nature as no reflections were observed in the patterns. Upon introducing a constant weight of 0.23 g of M-AG0.4, M-AG01 and M-AG02 for catalyzing the MB dye reduction reaction by NaBH<sub>4</sub>, the M-AG02 catalyst was found to be faster in its de-colorization. It was found that the Cu-AGxx and Co-AGxx had nearly similar performance when the effect of initial dye concentration and the effect of variation of the amount of the catalysts were tested in the MB dye reduction reaction. These results might be useful due to the simple preparation steps involved in the hydrogel support material.

#### Acknowledgment

This project was funded by the Deanship of Scientific Research (DSR) at King Abdulaziz University Jeddah, under grant no. G-472-130-38. The authors, therefore, acknowledge DSR with thanks for technical and financial support.

#### References

- [1] T. Kamal, S.B. Khan, A.M. Asiri, Nickel nanoparticles-chitosan composite coated cellulose filter paper: an efficient and easily recoverable dip-catalyst for pollutants degradation, *Environ. Pollut.*, 218 (2016) 625–633.
- [2] T. Kamal, I. Ahmad, S.B. Khan, A.M. Asiri, Synthesis and catalytic properties of silver nanoparticles supported on porous cellulose acetate sheets and wet-spun fibers, *Carbohydr. Polym.*, 157 (2017) 294–302.
- [3] S.B. Khan, F. Ali, T. Kamal, Y. Anwar, A.M. Asiri, J. Seo, CuO embedded chitosan spheres as antibacterial adsorbent for dyes, *Int. J. Biol. Macromol.*, 88 (2016) 113–119.
- [4] T. Kamal, S.B. Khan, S. Haider, Y.G. Alghamdi, A.M. Asiri, Thin layer chitosan-coated cellulose filter paper as substrate for immobilization of catalytic cobalt nanoparticles, *Int. J. Biol. Macromol.*, 104 (2017) 56–62.
- [5] T. Kamal, High performance NiO decorated graphene as a potential H<sub>2</sub> gas sensor, *J. Alloys Compd.*, 729 (2017) 1058–1063.
- [6] T. Kavitha, S. Haider, T. Kamal, M. Ul-Islam, Thermal decomposition of metal complex precursor as route to the synthesis of Co<sub>3</sub>O<sub>4</sub> nanoparticles: antibacterial activity and mechanism, *J. Alloys Compd.*, 704 (2017) 296–302.
- [7] C. Muhammad Tariq Saeed, S.K. Kh, K. Sher Bahadar, K. Tahseen, M.A. Abdullah, Synthesis and Pressure Sensing Properties of Pristine Zinc Oxide Nanopowder and its Blend with Carbon Nanotubes, *Curr. Nanosci.*, 12 (2016) 586–591.
- [8] T. Kamal, M. Ul-Islam, S.B. Khan, A.M. Asiri, Adsorption and photocatalyst assisted dye removal and bactericidal performance of ZnO/chitosan coating layer, *Int. J. Biol. Macromol.*, 81 (2015) 584–590.
- [9] I.Z. Awan, S.B. Hussain, A. ul Haq, A.Q. Khan, Wondrous Nanotechnology, *J. Chem. Soc. Pak.*, 38 (2016) 1026–1055.
- [10] F. Ali, S.B. Khan, T. Kamal, Y. Anwar, K.A. Alamry, A.M. Asiri, Bactericidal and catalytic performance of green nanocomposite based-on chitosan/carbon black fiber supported monometallic and bimetallic nanoparticles, *Chemosphere*, 188 (2017) 588–598.
- [11] I. Ahmad, S.B. Khan, T. Kamal, A.M. Asiri, Visible light activated degradation of organic pollutants using zinc-iron selenide, *J. Mol. Liq.*, 229 (2017) 429–435.
- [12] N. Sahiner, Soft and flexible hydrogel templates of different sizes and various functionalities for metal nanoparticle preparation and their use in catalysis, *Prog. Polym. Sci.*, 38 (2013) 1329–1356.
- [13] F. Ali, S.B. Khan, T. Kamal, Y. Anwar, K.A. Alamry, A.M. Asiri, Bactericidal and catalytic performance of green nanocomposite based-on chitosan/carbon black fiber supported monometallic and bimetallic nanoparticles, *Chemosphere*, 188 (2017) 588–598.
- [14] M. Ajmal, S. Demirci, M. Siddiq, N. Aktas, N. Sahiner, Simultaneous catalytic degradation/reduction of multiple organic compounds by modifiable p(methacrylic acid-co-acrylonitrile)-M (M: Cu, Co) microgel catalyst composites, *New J. Chem.*, 40 (2016) 1485–1496.
- [15] Z. Li, H. Sai, S.C. Warren, M. Kamperman, H. Arora, S.M. Gruner, U. Wiesner, Metal Nanoparticle-Block Copolymer Composite Assembly and Disassembly, *Chem. Mater.*, 21 (2009) 5578–5584.
- [16] A.K. Tiwari, S. Gangopadhyay, C.-H. Chang, S. Pande, S.K. Saha, Study on metal nanoparticles synthesis and orientation of gemini surfactant molecules used as stabilizer, *J. Colloid Interface Sci.*, 445 (2015) 76–83.
- [17] I. Ahmad, T. Kamal, S.B. Khan, A.M. Asiri, An efficient and easily retrievable dip catalyst based on silver nanoparticles/chitosan-coated cellulose filter paper, *Cellulose*, 23 (2016) 3577–3588.
- [18] L.A. Shah, J. Ambreen, I. Bibi, M. Sayed, M. Siddiq, Silver Nanoparticles Fabricated Hybrid Microgels for Optical and Catalytic Study, *J. Chem. Soc. Pak.*, 38 (2016) 850–858.
- [19] M. Thomas, G.A. Naikoo, M.U.D. Sheikh, M. Bano, F. Khan, Effective photocatalytic degradation of Congo red dye using alginate/carboxymethyl cellulose/TiO<sub>2</sub> nanocomposite hydrogel under direct sunlight irradiation, *J. Photochem. Photobiol. A*, 327 (2016) 33–43.
- [20] H. Firouzabadi, N. Iranpoor, M. Gholinejad, F. Kazemi, Agarose hydrogel as an effective bioorganic ligand and support for the stabilization of palladium nanoparticles. Application as a recyclable catalyst for Suzuki-Miyaura reaction in aqueous media, *RSC Adv.*, 1 (2011) 1013–1019.
- [21] K. Shahid Ali, K. Sher Bahadar, K. Tahseen, M.A. Abdullah, A. Kalsoom, Recent Development of Chitosan Nanocomposites for Environmental Applications, *Recent Pat. Nanotechnol.*, 10 (2016) 181–188.
- [22] T. Kamal, S.B. Khan, A.M. Asiri, Synthesis of zero-valent Cu nanoparticles in the chitosan coating layer on cellulose microfibrils: evaluation of azo dyes catalytic reduction, *Cellulose*, 23 (2016) 1911–1923.

- [23] K. Tahseen, A. Nauman, A.N. Abbas, B.K. Sher, M.A. Abdullah, Polymer Nanocomposite Membranes for Antifouling Nanofiltration, *Recent Pat. Nanotechnol.*, 10 (2016) 189–201.
- [24] M. Sameer Ahmed, T. Kamal, S.A. Khan, Y. Anwar, M.T. Saeed, A. Muhammad Asiri, S. Bahadar Khan, Assessment of Antibacterial Ni-Al/chitosan Composite Spheres for Adsorption Assisted Photo-Degradation of Organic Pollutants, *Curr. Nanosci.*, 12 (2016) 569–575.
- [25] S.A. Khan, S.B. Khan, T. Kamal, M. Yasir, A.M. Asiri, Antibacterial nanocomposites based on chitosan/Co-MCM as a selective and efficient adsorbent for organic dyes, *Int. J. Biol. Macromol.*, 91 (2016) 744–751.
- [26] A.H. Khani, A.M. Rashidi, G. Kashi, Synthesis of tungsten nanoparticles by reverse micelle method, *J. Mol. Liq.*, 241 (2017) 897–903.
- [27] S.M. El-Sheikh, A.A. Ismail, J.F. Al-Sharab, Catalytic reduction of p-nitrophenol over precious metals/highly ordered mesoporous silica, *New J. Chem.*, 37 (2013) 2399–2407.
- [28] J.-P. Deng, W.-C. Shih, C.-Y. Mou, Electron Transfer-Induced Hydrogenation of Anthracene Catalyzed by Gold and Silver Nanoparticles, *J. Phys. Chem. C*, 111 (2007) 9723–9728.
- [29] S. Butun, N. Sahiner, A versatile hydrogel template for metal nano particle preparation and their use in catalysis, *Polymer*, 52 (2011) 4834–4840.
- [30] N. Sahiner, S. Sagbas, N. Aktas, Very fast catalytic reduction of 4-nitrophenol, methylene blue and eosin Y in natural waters using green chemistry: p(tannic acid)-Cu ionic liquid composites, *RSC Adv.*, 5 (2015) 18183–18195.
- [31] C. Yang, W. Dong, G. Cui, Y. Zhao, X. Shi, X. Xia, B. Tang, W. Wang, Highly-efficient photocatalytic degradation of methylene blue by PoPD-modified TiO<sub>2</sub> nanocomposites due to photosensitization-synergetic effect of TiO<sub>2</sub> with PoPD, *Sci. Rep.*, 7 (2017) 3973.
- [32] F. Ali, S.B. Khan, T. Kamal, K.A. Alamry, A.M. Asiri, T.R.A. Sobahi, Chitosan coated cotton cloth supported zero-valent nanoparticles: simple but economically viable, efficient and easily retrievable catalysts, *Sci. Rep.*, 7 (2017) 16957.
- [33] B.-Z. Lin, X.-L. Li, B.-H. Xu, Y.-L. Chen, B.-F. Gao, X.-R. Fan, Improved photocatalytic activity of anatase TiO<sub>2</sub>-pillared HTaWO<sub>6</sub> for degradation of methylene blue, *Microporous Mesoporous Mater.*, 155 (2012) 16–23.

## Supplementary figure

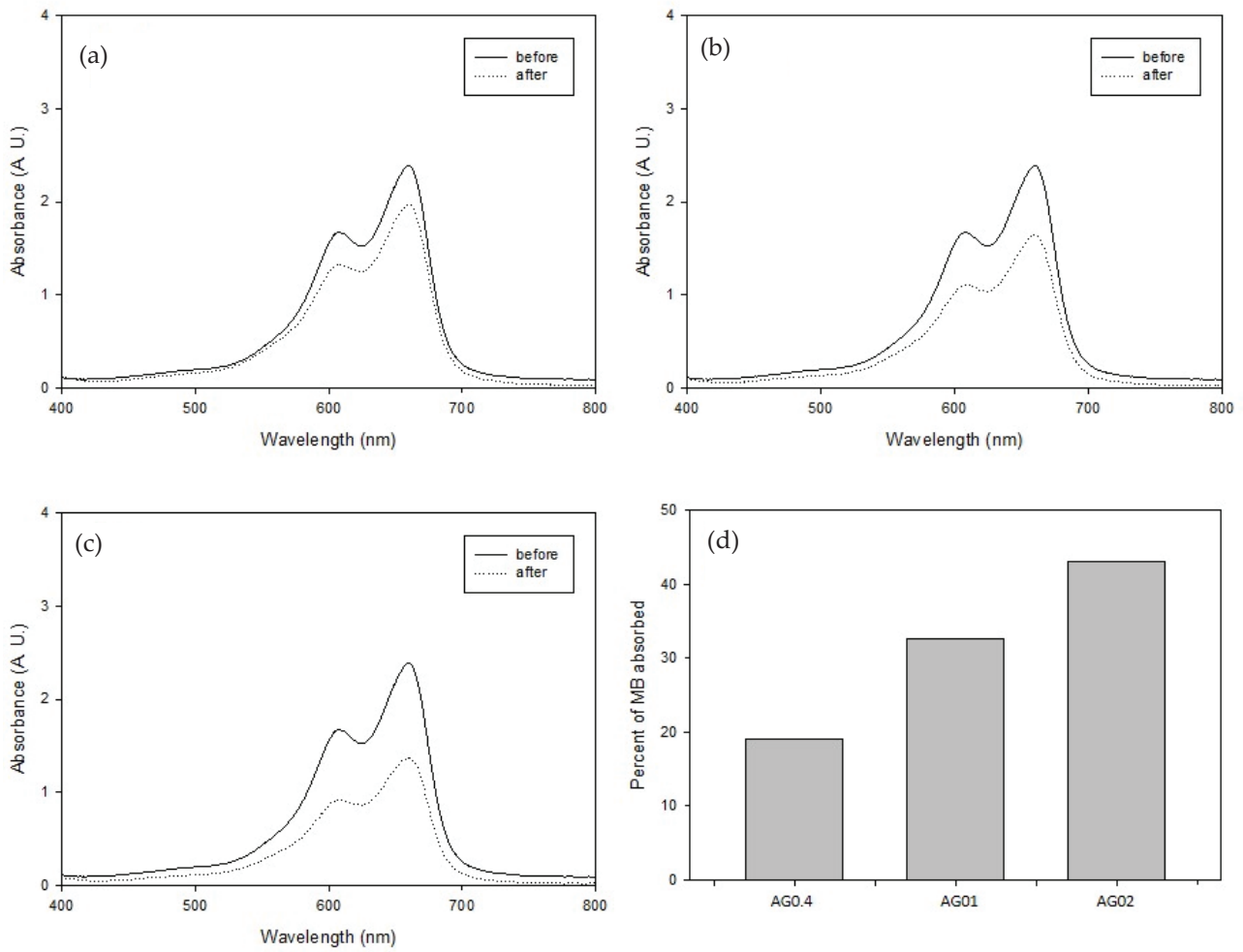


Fig. S1. UV-visible absorbance spectra of MB aqueous solution in the presence of (a) AG0.4, (b) AG01 and (c) AG02. (d) Percent adsorption of the MB on the gels. Each panel in (a)–(c) has two spectra which were recorded before and after the addition of the gels.